7236–7247 Nucleic Acids Research, 2010, Vol. 38, No. 20 Published online 3 July 2010
doi:10.1093/nar/gkq599

Small nucleolar RNA interference in *Trypanosoma brucei*: mechanism and utilization for elucidating the function of snoRNAs

Sachin Kumar Gupta[1], Avraham Hury[1], Yaara Ziporen[1], Huafang Shi[2], Elisabetta Ullu[2,3] and Shulamit Michaeli[1,*]

[1]The Mina and Everard Goodman Faculty of Life Sciences and Advanced Materials and Nanotechnology Institute, Bar-Ilan University, Ramat-Gan 52900 Israel, [2]Department of Internal Medicine and [3]Department of Cell Biology, Yale University Medical School, New Haven, CT 06536-0812, USA

Received November 30, 2009; Revised June 16, 2010; Accepted June 17, 2010

ABSTRACT

Expression of dsRNA complementary to small nucleolar RNAs (snoRNAs) in *Trypanosoma brucei* results in snoRNA silencing, termed snoRNAi. Here, we demonstrate that snoRNAi requires the nuclear *Tb*DCL2 protein, but not *Tb*DCL1, which is involved in RNA interference (RNAi) in the cytoplasm. snoRNAi depends on Argonaute1 (Slicer), and on *Tb*DCL2, suggesting that snoRNA dicing and slicing takes place in the nucleus, and further suggesting that AGO1 is active in nuclear silencing. snoRNAi was next utilized to elucidate the function of an abundant snoRNA, TB11Cs2C2 (92 nt), present in a cluster together with the spliced leader associated RNA (SLA1) and snR30, which are both H/ACA RNAs with special nuclear functions. Using AMT-UV cross-linking and RNaseH cleavage, we provide evidence for the interaction of TB11Cs2C2 with the small rRNAs, srRNA-2 and srRNA-6, which are part of the large subunit (LSU) rRNA. snoRNAi of TB11Cs2C2 resulted in defects in generating srRNA-2 and LSUβ rRNA. This is the first snoRNA described so far to engage in trypanosome-specific processing events.

INTRODUCTION

RNA interference (RNAi) in *Trypanosoma brucei* was one of the first dsRNA-mediated silencing systems described in eukaryotes (1); since its discovery, RNAi has become one of the most useful tools for elucidating the function of protein coding genes in these organisms. In *T. brucei*, the natural RNAi pathway down-regulates transcripts from the retroposons, SLACS and INGI (2–4), and from a family of 147 bp chromosomal internal repeats, termed CIR 147 (5), which are present in a subset of putative centromeric regions (6). The nature of the target transcripts suggests that one major function of RNAi in *T. brucei* is to promote genome stability, though RNAi may also have a role in chromosome segregation (2,7,8).

The 'classical' RNAi pathway, which is triggered by long dsRNA, is mediated by two key enzymes, Dicer, an enzyme of the RNase III family, and Slicer, a member of the Argonaute (AGO) protein family with an RNase H-type fold (9). Trypanosomes, like yeast, possess a single Argonaute (AGO1) homolog (2,10), but, unlike yeast, express two Dicer-like (DCL) proteins, *Tb*DCL1 (3) and *Tb*DCL2 (3,5). *Tb*DCL1 is cytoplasmic and mediates the cytoplasmic RNAi response, which is harnessed in experimental RNAi to induce mRNA degradation. In contrast, *Tb*DCL2, which is mostly nuclear (5), is central for dicing both retroposon and repeat-derived dsRNA and provides the first line of defense against these potentially dangerous molecules in the nucleus. On the other hand, both *Tb*DCL1 and *Tb*DCL2 contribute to the generation of retroposon-derived small interfering RNAs (siRNAs), suggesting that the two DCL proteins have both distinct and shared functions.

The existence of a nuclear phase of RNAi was also suggested by our previous studies demonstrating downregulation of small nucleolar RNAs (snoRNAs), triggered by expression of anti-sense RNA from an episomal vector in the monogenetic trypanosomatid, *Leptomonas collosoma*. This process was termed snoRNAi (11). We showed that snoRNAi in *L. collosoma*

*To whom correspondence should be addressed. Tel: +972 3 5318068; Fax: +972 3 7384058; Email: michaes@mail.biu.ac.il

The authors wish it to be known that, in their opinion, the first three authors should be regarded as joint First Authors.

targets the mature snoRNA, but not its precursor, and we further provided evidence for the accumulation of siRNAs in snoRNAi-silenced cells. In *T. brucei* snoRNAi was achieved by expressing snoRNA information using a tetracycline inducible vector equipped with opposing T7 RNA polymerase (pol) promoters (11). Since the discovery of snoRNAi in trypanosomatids, the efficient silencing by siRNAs of telomerase RNA and 7SK RNA, two nuclear small RNAs, was reported, suggesting that nuclear RNAs can be down-regulated by RNAi in mammals, as well (12).

snoRNAs are one of the most abundant families of non-coding RNAs in eukaryotic genomes. Eukaryotic rRNA undergo both processing and extensive covalent modification that require the function of snoRNAs (13–16). The modifications include methylation of the 2′-hydroxyl residue (2′-*O*-methylation, Nm) (17) and isomerization of the uracil to pseudouridine (18,19). The snoRNAs guide these modifications following site-specific base-pairing with their targets. The snoRNAs that guide these modifications are designated by their specific sequence motifs: C/D boxed RNAs guide Nm, and H/ACA RNAs guide pseudouridylation (17–19). The C/D box RNAs, which are most relevant for this study, have 10–22 nt sequences of perfect complementarity to the sequences within the mature rRNA (20).

Recent genomic and functional studies revealed a very rich repertoire of snoRNAs in trypanosomes. Initial studies identified 21 clusters encoding 57 C/D snoRNAs and 34 H/ACA-like RNAs (21). Additional C/D snoRNAs were identified after partially mapping Nms on rRNA (22). An algorithm designed to identify the trypanosome single hairpin H/ACA-like RNA species carrying an AGA box at the 3′-end, identified additional H/ACA RNAs in *T. brucei* (23). At present, 46 H/ACA have been identified in *T. brucei* that have homologs in the other trypanosomatid species (24).

rRNA processing in trypanosomes differs from maturation in most eukaryotes. The small subunit (SSU) rRNA in trypanosomes is the largest known so far, and the large subunit (LSU) rRNA is processed into six fragments, two large ones termed LSUα and LSUβ rRNAs, and four small fragments, termed the small rRNA (srRNA) (25–27). The only trypanosome snoRNAs involved in rRNA maturation identified to date are U3, snR30 and MRP RNAs (22,28,29). Several of the snoRNAs shown to function in rRNA processing in other eukaryotes, including U22, U8, U14, have not been identified to date in trypanosomes (20).

In this study, we examined the mechanism of snoRNAi in *T. brucei,* and found that silencing of the TB11Cs2C2 snoRNA requires *Tb*DCL2, since co-silencing of TB11Cs2C2 and *Tb*DCL2 nearly abolished snoRNAi. No effect on snoRNAi was observed in cells expressing a dominant negative *Tb*DCL1 allele, previously shown to inhibit the cytoplasmic RNAi response (3). snoRNAi was also compromised in cells silenced for AGO1, suggesting that the snoRNAi requires the function of both *Tb*AGO1 and *Tb*DCL2. snoRNAi was then used to investigate the function of TB11Cs2C2 snoRNA, one of the most abundant snoRNA forms in trypanosomes, and previously implicated in methylation of LSU rRNA (30). Here, we demonstrate the interaction between TB11Cs2C2 and its targets using *in vivo* UV-induced AMT cross-linking. SnoRNAi of TB11Cs2C2 suggests that this RNA is involved in rRNA processing of LSUβ to release the small rRNA fragments, srRNA-2 and -6. This is the first snoRNA described to date that mediates trypanosome-specific rRNA processing events. The function of the neighboring TB11CsC1 snoRNA was also elucidated, and this snoRNA is implicated in processing of SSU rRNA. This study suggests that snoRNAi operates in the nucleus utilizing *Tb*DCL2 and *Tb*AGO1, and this process can be harnessed to elucidate the function of nuclear/nucleolar non-coding RNAs.

MATERIALS AND METHODS

All the oligonucleotides used in this study are listed in Supplementary Figure S1.

Cell culture, constructs and transfection

Procyclic *T. brucei* strain 29–13 which carries integrated genes for T7 polymerase and the tetracycline repressor was grown in SDM-79 medium supplemented with 10% foetal calf serum in the presence of 50 μg/ml hygromycin and 15 μg/ml G418. The T7 RNA pol opposing silencing constructs were prepared as previously described (31) using oligonucleotides listed in Supplementary Data S1. Cells were transfected and clonal populations were obtained in microtiter plates, as previously described (32).

Northern blot analysis

Total RNA was prepared with TRI-Reagent (Sigma), and 20 μg/lane were fractionated on a 1.2% agarose, 2.2 M formaldehyde gel. The RNA was visualized with ethidium bromide. The *Tb*DCL2 and SmD3 mRNAs were detected using a randomly labeled probe (Random Primer DNA Labeling Mix, Biological Industries Ltd.). For analyzing snoRNAs and siRNAs, total RNA (10 μg) was fractionated on a 10% polyacrylamide gel containing 7 M urea. The RNA was transferred to a nylon membrane (Hybond; Amersham Biosciences), and probed with an anti-sense RNA probe specific to the gene.

RNA probes

RNA probes were synthesized on a PCR template generated using primers described in Supplementary Table S1, and containing the T7 polymerase promoter sequence.

Primer extension and RNase protection analyses

RNA was prepared from *T. brucei* cells using the TRI-Reagent (Sigma). Primer extension analysis was performed as described (33,34) using 5′-end-labeled oligonucleotides specific to each target RNA. The extension products were analyzed on a 6% polyacrylamide/7 M urea gel and visualized by autoradiography. Total RNA was prepared and analyzed by the RNase protection

assay, as previously described (32). The RNase protection assay products were separated on 6% polyacrylamide/7 M urea gels and visualized by autoradiography. To calculate differences in the level of extension products, the films were subjected to densitometric analysis using ImageJ.

AMT, *in vivo* UV cross-linking

Cross-linking was performed essentially as described in (35). Briefly, *T. brucei* cells were harvested at 1×10^7 cells/ml and washed twice with PBS. Cells ($\sim 10^9$) were concentrated and incubated on ice. 4′-Aminomethyl–trioxsalen hydrochloride (AMT) (Sigma) was added to the cells at a concentration of 0.2 mg/ml. Cells treated with AMT were kept on ice and irradiated using a UV lamp at 365 nm at a light intensity of 10 μW/cm^2 for 30 min. Next, the cells were washed once with PBS and deproteinized by digestion with proteinase K (Roche) (200 μg/ml in 1% SDS for 60 min). RNA was prepared using TRI-Reagent (Sigma).

Affinity purification of snoRNAs using a complementary 2′-*O*-methyl biotinylated oligonucleotides

First, 250 μg of RNA extracted from UV treated cells (+UV) and untreated cells (–UV), in hybridization buffer (20 mM HEPES pH 8, 5 mM $MgCl_2$, 300 mM KCl, 0.01% NP40, 1 mM DTT) was heated for 2 min at 80°C and then chilled on ice. Oligonucleotides linked to biotin (Figure S1) (8 μg) were added, and the solution was incubated overnight at room temperature. Next, 50 μl of blocked Neutravidin Sepharose beads (Pierce) were added, and the reaction was incubated for 2 h at 4°C. Blocking of the beads was performed in 1 ml blocking buffer [700 μl DEPC treated water, 200 μl WB100 (20 mM HEPES pH 8, 10 mM $MgCl_2$, 100 mM KCl, 0.01% NP40 (v/v), 1 mM DTT), 50 μl BSA (10 mg/ml), 10 μl Glycogen (20 mg/ml), 40 μl tRNA (11 mg/ml)]. After binding of the RNA to the oligonucleotide-bound beads, the beads were washed five times in WB400 buffer [20 mM HEPES pH 8, 10 mM $MgCl_2$, 400 mM KCl, 0.01% NP40(v/v), 1 mM DTT]. RNA was eluted from the beads using the TRI-Reagent (Sigma) and analyzed by primer extension (For TB11Cs2C2) or by RT–PCR (for TB11Cs2C1).

RNaseH cleavage and splint labeling

RNase H cleavage of rRNA was performed by annealing 200 pmol of oligonucleotides as indicated in the figures (see Supplementary Figure S1 for specific primer sequences) with 20 μg of total RNA at 65°C for 10 min in 75 mM KCl, 50 mM Tris–HCl (pH 8.3), 3 mM $MgCl_2$, 10 mM DTT. The samples were then placed on ice and two units of RNase H (NEB) were added. The samples were further incubated at 37°C for 60 min, phenol/chloroform extracted, and ethanol precipitated. Samples were then subjected to splint labeling. For splint labeling, the RNA (10–20 μg) was mixed with 150 pmol of oligonucleotide (see Supplementary Data S1 for primer sequence) and heated for 2 min at 85°C in 50 mM Tris–HCl (pH 7.8), 10 mM $MgCl_2$ and 1 mM DTT. The annealing reaction was quenched on ice for 30 min; 50 μCi of [α-^{32}P]-dCTP (3000 Ci/mmol) and five units of T7 DNA polymerase (Sequenase V. 2.0, USB) were then added, and the reaction was incubated for 1 h at 37°C. RNA was separated on a 6% polyacrylamide–7 M urea gel.

RT–PCR

The RNA was treated with the 'DNase-free' reagent (Ambion) according to the manufacturer's protocol for 30 min to remove DNA contamination. Reverse transcription was performed by random priming (Reverse transcription system, Promega). The samples were heated for 5 min at 70°C, followed by chilling on ice for 5 min. Next, one unit of AMV-reverse transcriptase (Promega) was added, together with one unit RNase inhibitor (Promega) and the elongation reaction was performed according to the manufacturer's instructions at 25°C for 10 min and then at 42°C for 60 min (Promega kit). The cDNA was used for PCR amplification using primers as specified in Supplementary Table S1. The cDNA was diluted to enable exponential amplification by PCR as determined by different dilutions of the cDNA. For rRNA analysis, the cDNA was prepared from ~1 μg RNA, and was diluted ~1:500 for PCR amplification. To map the cross-linked adducts on rRNA, RNA obtained from AMT-UV cross-linking (250 μg) after affinity selection was used to prepare cDNA, and the cDNA was diluted ~1:50. PCR was performed on 1 μl of the diluted cDNA (described above), with the addition of 1 μM primers and ReadyMix^{TM} Taq PCR Reaction Mix with $MgCl_2$ (Sigma). The PCR conditions were as follows: 95° for 2 min, followed by 25 cycles of 95° for 30 s, 60° for 30 s and 72° for 30 s.

RESULTS

RNAi of TB11Cs2C2 snoRNA requires the nuclear Dicer, *Tb*DCL2, but not the cytoplasmic Dicer, *Tb*DCL1

The snoRNA TB11Cs2C2 (92 nt) is located in a cluster that includes SLA1, which guides pseudouridylation on the SL RNA (36,37), the snR30 homolog, which participates in rRNA processing (29), and another C/D snoRNA species, TB11Cs2C1 (76 nt). The C/D snoRNAs TB11Cs2C1/C2 were implicated in guiding modifications on rRNA by non-conventional guiding rules (30). However, the methylation predicted to be modified by TB11Cs2C1 (30) is guided by another snoRNA (TB9Cs2C4) based on the conventional +5 rule that governs the methylation of all trypanosome snoRNAs (21,38). As opposed to the snoRNAs that guide modification, TB11Cs2C1/C2 are very abundant, like the U3 snoRNA (22). SnoRNAs are known to either guide modification, to function in rRNA processing, or to perform both functions.

In this study, we utilized snoRNAi of TB11Cs2C2 as a model both for elucidating the mechanism of snoRNAi and to investigate the possible role of this RNA in rRNA processing.

First, we examined which of the Dicers, *Tb*DCL1 and/or *Tb*DCL2, is essential for snoRNAi. The TB11Cs2C2 gene was cloned into the pZJM vector,

expressing dsRNA from two T7 RNA pol opposing promoters (31). The construct was used to transfect parental cells, cells carrying a dominant negative *Tb*DCL1 mutant (3), and a cell line silenced for *Tb*DCL2. The dominant-negative *Tb*DCL1 mutant was expressed as Tet-inducible ectopic copy carrying a dual BB2/FLAG tag and a base substitution of aspartate to glycine at amino acid 966 (3). This mutant is defective in cytoplasmic RNAi triggered by transfection of α-tubulin dsRNA, however its specific mode of action has not been investigated further (3). The results in Figure 1A–a demonstrate that, a cell line carrying the silencing construct for TB11Cs2C2 expressed the FLAG-tagged dominant-negative *Tb*DCL1 upon tetracycline induction. To examine the phenotype of dominant-negative *Tb*DCL1 and to verify that this mutant is defective in cytoplasmic RNAi, two cell lines were generated using the pZJM vector expressing dsRNA to silence SmD3 from the two T7 opposing promoters (31). One cell line contained the SmD3 silencing construct, and the second cell line contained both the SmD3 silencing construct as well as the dominant-negative *Tb*DCL1. The results (Figure 1A-b) demonstrate that the presence of the dominant-negative *Tb*DCL1 perturbed the silencing of SmD3 (compare lanes 2–4). Next, the *Tb*DCL2 (Tb927.3.1230) was silenced by RNAi as described in 'Materials and methods' section, using the pZJM vector, described above (31). After establishing a clonal cell population, we introduced the silencing construct for TB11Cs2C2, carrying the blasticidin resistance gene. The silencing of *Tb*DCL2 was confirmed by northern analysis (Figure 1A-c), as well as by demonstrating reduction in the level of CIR147 siRNAs (Figure 1A-d), whose production depends on *Tb*DCL2 (5).

After confirming that silencing of *Tb*DCL2 was efficient, the silencing of the TB11Cs2C2 snoRNA was examined by primer extension. The results, shown in Figure 1B and Supplementary Figure S2(A), quantitated by densitometric analysis, demonstrate that induction of TB11Cs2C2 silencing in parental cells reduced the level of the snoRNA by 80% (compare lanes 1 and 2). Similarly, the dominant-negative *Tb*DCL1 mutant did not interfere

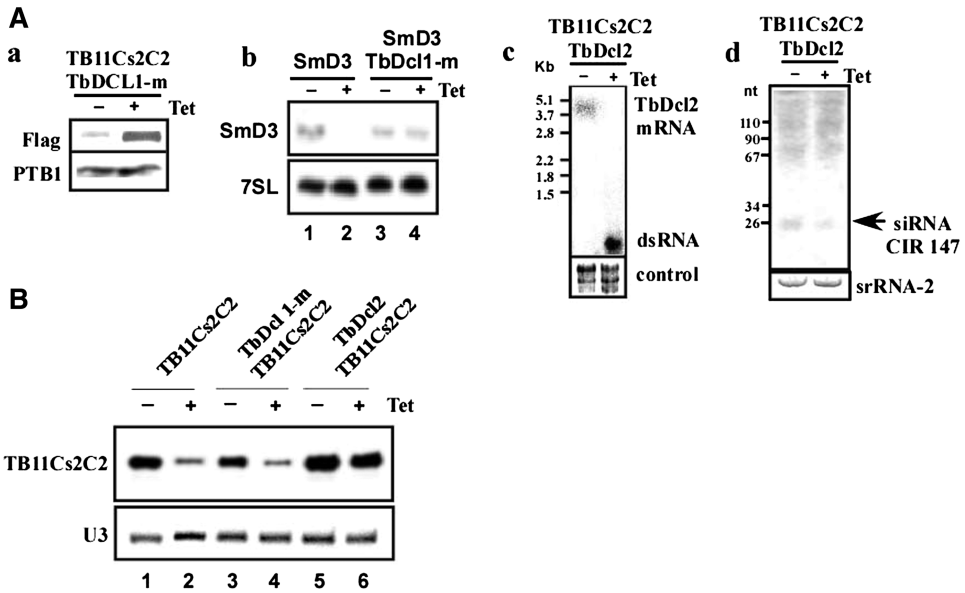

Figure 1. *Tb*DCL2 but not *Tb*DCL1 is essential for snoRNAi. (**A**) (**a**) Western blot analysis demonstrating the expression of DCL1-m carrying a FLAG tag. A whole cell lysate was prepared from 10^8 cells and the blot was reacted with a monoclonal anti-flag M2 antibody (Sigma). Equal loading was confirmed using anti-PTB antibodies (48). (**b**) Northern analysis of cells carrying the silencing constructs for SmD3 and TbDCl1-m. RNA was prepared from uninduced cells (–Tet) and cells after 3 days of induction (+Tet). Total RNA (20 μg/lane) was subjected to northern blot analysis with random-labeled probes. The transcripts examined are indicated. Lanes 1 and 2, RNA was prepared from uninduced cells, or after induction, from cells carrying the SmD3 silencing construct. Lanes 3, 4, the same as 1, 2 but from cells carrying both the silencing construct and the TbDCl1 mutation. The level of 7SL RNA was used to control for equal loading. (**c**) Northern analysis of cells carrying the silencing constructs for TB11Cs2C2 and *Tb*DCL2. Northern blot analysis of *Tb*DCL2 mRNA after silencing. RNA was prepared from uninduced cells (–Tet) and cells after 3 days of induction (+Tet). Total RNA (20 μg/lane) was subjected to northern blot analysis with random-labeled probes. The transcripts examined are indicated. The rRNA level was examined by ethidium bromide staining and was used as a control for loading. Hybridization with rRNA probe was used and the sizes of mature and pre-rRNA were used as marker. (**d**) Northern analysis to determine the level of CIR147 under *Tb*DCL2 silencing. RNA was prepared from uninduced cells (–Tet), and cells after 3 days of induction (+Tet). The RNA was separated on a 10% denaturing gel, and after electrotransfer, the membrane was hybridized with an RNA probe complementary to CIR147. pBR322 DNA-*Msp I* digest was used as a size marker. The position of the siRNAs and the identity of the RNAs are indicated. (**B**) The level of TB11Cs2C2 snoRNA in cells expressing the *Tb*DCL1 dominant negative allele, and under *Tb*DCL2 silencing. RNA was prepared from the different cell lines, before induction (–Tet), and after induction (+Tet), and subjected to primer extension with oligonucleotide complementary to 3′-end of TB11Cs2C2. The products were separated on a 7 M urea denaturing gel. Primer extension with anti-U3 specific probes was used to confirm equal loading. The identity of the RNAs and the cell lines are indicated. Lanes 1 and 2, RNA from parental cells carrying the silencing construct of TB11Cs2C2 (–Tet), and after 3 days of induction (+Tet); lanes 3 and 4, the same as in lanes 1 and 2, but the cells carried the *Tb*DCL1 mutant and the silencing construct for TB11Cs2C2; lanes 5 and 6, as the previous lanes, but the cells carried the silencing construct for TB11Cs2C2 and a T7 RNA pol opposing promoter construct to silence DCL2.

with snoRNAi, since the level of snoRNA was also reduced by 85% upon tetracycline induction (compare lanes 3 and 4). However, when snoRNAi was examined under depletion of *Tb*DCL2, only a minor reduction was observed in the snoRNA level, suggesting that *Tb*DCL2 but not *Tb*DCL1 is essential for snoRNAi.

Argonaute is essential for snoRNAi

To examine if, as in cytoplasmic RNAi, both Dicer and Argonaute are necessary to execute the silencing, the effect of *Tb*AGO1 silencing on snoRNAi was examined. *Tb*AGO1 was silenced using a T7 RNA pol opposing construct (31). Cell lines silenced for *Tb*AGO1 were then transfected with the silencing construct for TB11Cs2C2, and a stable clonal cell line was established and further characterized. The western blot analysis presented in Figure 2A indicated that the *Tb*AGO1 level was significantly reduced in this cell line, suggesting the efficient silencing of *Tb*AGO1 in cells expressing the silencing constructs for both *Tb*AGO1 and TB11Cs2C2. Next, the level of the snoRNA was examined by primer extension in the different cell lines. The results, shown in Figure 2B (lanes 1 and 2) and Supplementary Figure S2(B), demonstrate that silencing of snoRNA is compromised in cells silenced for *Tb*AGO1. As a control, silencing of TB11Cs2C2 in the parental strain was examined (lanes 3 and 4). Thus, the results shown in Figures 1 and 2 suggest that snoRNAi requires both *Tb*AGO1 and *Tb*DCL2.

TB11Cs2C2 is a snoRNA that interacts by base-pairing with srRNA-2 and srRNA-6

As mentioned above, several findings suggest that TB11Cs2C2 is likely to have a special function in rRNA processing: it is located in a cluster whose members are abundant RNAs with functions other than rRNA modification; it is not involved in methylation, as was initially proposed (30); and it is as abundant as U3 snRNP, which functions in rRNA processing (22).

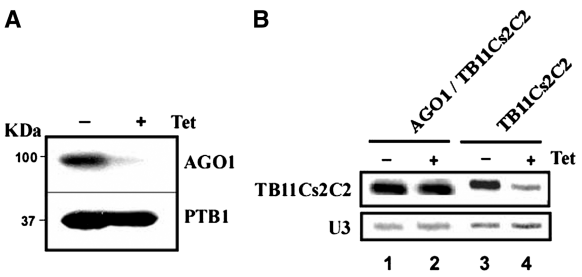

Figure 2. AGO1 is essential for snoRNAi. (**A**) Western blot analysis demonstrating the depletion of AGO1. A whole-cell lysate was prepared from 10^8 cells, and the blot was reacted with anti-AGO1 antibodies. Equal loading was confirmed by reactivity with anti-PTB1 antibodies. (**B**) Primer extension demonstrating the dependence of snoRNAi on *Tb*AGO1. RNA was prepared before silencing (–Tet) or after 3 days of silencing (+Tet), and was examined by primer extension. Primer extension of U3 snoRNA was used to control for equal loading. The identities of the RNA species and the cell lines are indicated. Lanes 1 and 2, RNA from cells expressing both the silencing construct for AGO1 and TB11Cs2C2 before and after 3 days of induction; lanes 3 and 4, the same as in lanes 1 and 2, but the cells carried the silencing construct for TB11Cs2C2.

To elucidate the function of this snoRNA, a bioinformatic search was conducted to identify potential targets. The entire rRNA cluster (GenBank AL929603.2) was analyzed by BLAST to identify potential base-pair interactions between the snoRNA and rRNA. Four potential base-pair interaction domains with rRNA were found; two sites with extensive complementarity between TB11Cs2C2 and the coding region of srRNA-2 and -6 (see Figure 4A for a schematic representation of the rRNA locus) and two weak interactions in ITS6 and ITS7 (not presented). The potential interactions between TB11Cs2C2 and srRNA-2 and -6 are depicted in Figure 3A and B. Based on this model, different domains of TB11Cs2C2 are involved in base-pair interaction with each of the targets. The secondary structure of TB11Cs2C2 is in agreement with the canonical structure of C/D snoRNA (20). In addition, a stem-loop structure is situated upstream to the interaction domain with srRNA-6. The validity of this structure is supported by phylogenic conservation among the trypanosomes (*T. brucei, T. vivax and T. cruzi*). Sequence differences that exist among the trypanosomatids include compensatory changes that maintain both the structure of the stems as well as the predicted base-pairing with the rRNA targets (Figure 3A).

To obtain biochemical evidence for these interactions, we carried out AMT treatment followed by UV cross-linking. AMT compounds are unique in their ability to freeze helical regions of nucleic acids. First, the planar AMT molecule intercalates within the double-helical region; upon irradiation at 365 nm, covalent adducts with pyrimidine bases are formed (39). This method was used previously in trypanosomes to identify interactions between the spliced leader RNA and other small RNA species (35,40). AMT intercalates within stems formed either inter- or intra-molecularly. To identify intermolecular interactions, a protocol was devised to enrich the cross-linked adducts by affinity selection using an anti-sense biotinylated oligonucleotide complementary to TB11Cs2C2. After affinity selection, the adducts were mapped on TB11Cs2C2 by primer extension (note that reverse transcriptase usually stops one nucleotide before the cross-linked site). Only adducts that were enriched by the affinity selection were considered to have resulted from the interaction between TB11Cs2C2 and rRNA. To evaluate intramolecular cross-links, total RNA was extracted from AMT-treated cross-linked cells, separated on a denaturing gel, and the RNA band corresponding to the size of TB11Cs2C2 was excised and used to map the cross-linked adducts. This RNA should only contain intramolecular cross-linked adducts but not intermolecular cross-linked sites. Thus, primer extension stops common to lanes 4 and lane 6 in Figure 3C are the result of intramolecular cross-linking. These stops are marked with white arrowheads (Figure 3C) and are circled on the secondary structure diagram, and filled in gray (Figure 3A). The adducts were mapped to the proposed stems, supporting the proposed secondary structure of the molecule. In the unique stem located between positions 21 and 49 nt of the RNA, four intermolecular cross-linked adducts were detected (U24, U34, U41, U47) and a single

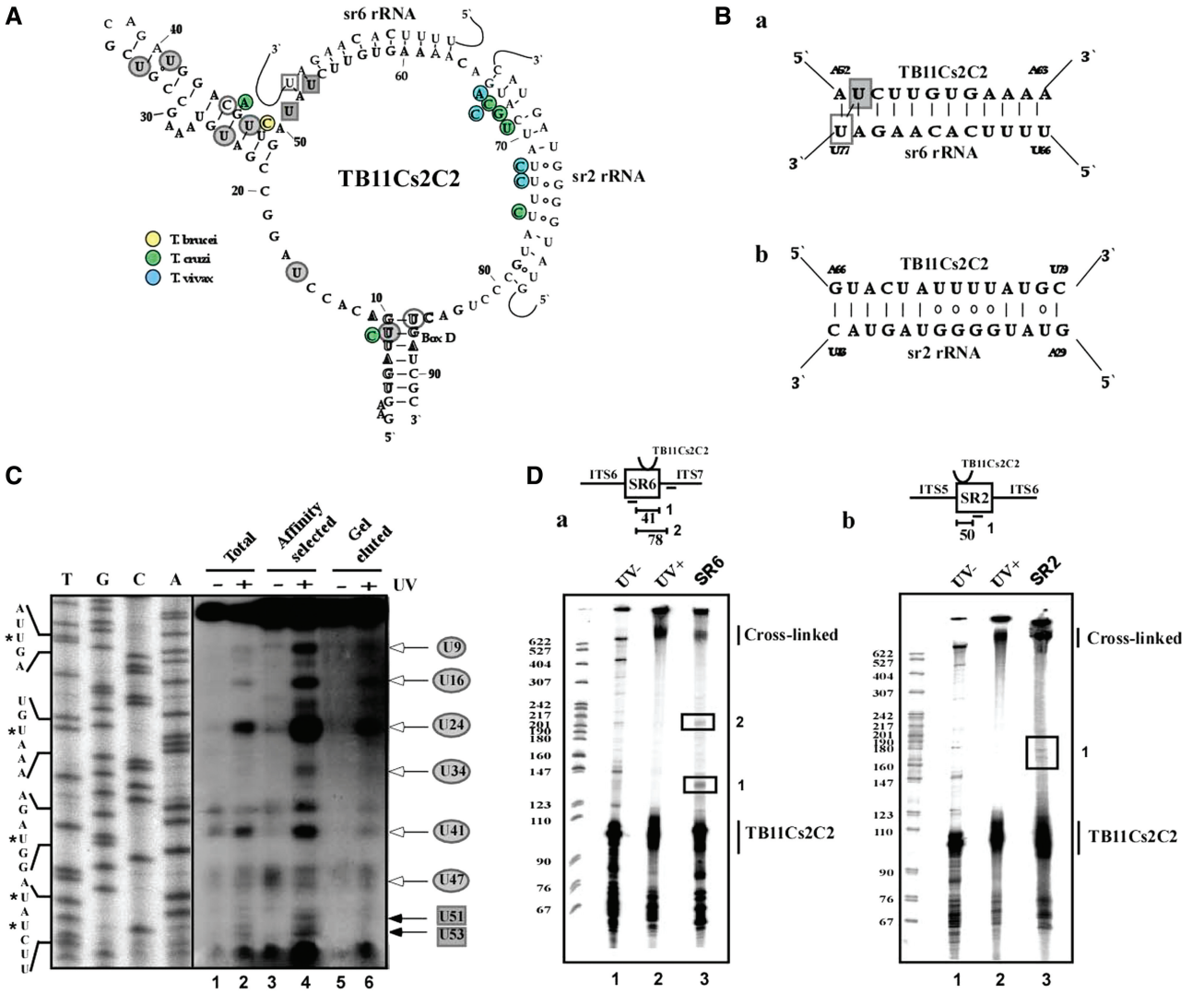

Figure 3. Potential interactions of TB11Cs2C2 snoRNA with rRNA. (**A**) The predicted secondary structure of TB11Cs2C2. The structure is presented showing potential interactions with small rRNA-2 and -6. The intramolecular cross-linked sites are circled and filled in gray, and the intermolecular site is boxed. Changes in the sequence compared to *T. brucei* are circled; green and turquoise represent *T. cruzi* and *T. vivax*, respectively. The yellow circles indicate changes in *T. brucei* between the sequence in the different repeats. (**B**) Potential base-pair interaction between srRNA and TB11Cs2C2. (**a**) interaction with srRNA-6; and (**b**) interaction with srRNA-2. The positions on both RNAs are indicated; the intramolecular cross-linked adducts are boxed. (**C**) Primer extension to map the AMT-adducts on TB11Cs2C2. Cells (10^{10}) were treated with AMT and irradiated with UV light at 365 nm with an intensity of 10 μW/cm^2 for 60 min. RNA was prepared from irradiated cells and from control untreated cells and subjected to affinity selection using a 2′-*O*-methyl biotinylated oligonucleotide complementary to TB11Cs2C2. RNA from the different samples was subjected to primer extension with a primer complementary to TB11Cs2C2. Lanes 1, 3, 5: RNA was derived from the same step of purification but was extracted from untreated control cells. Lane 2, total RNA (10 μg) from treated cells. Lane 4, affinity selected RNA prepared as specified in 'Materials and Methods' section. Lane 6, RNA (~90 nt) from cells treated with AMT and subjected to UV cross-linking eluted from a preparative gel as described in 'Materials and Methods' section. The extension products were separated on a 6% denaturing gel. The different treatments are indicated above the lanes. DNA sequencing of the clone carrying the TB11Cs2C2 gene with the same primer was used for mapping the adducts, and is given in the opposite orientation to correspond with the coding sequence of the RNA, indicated on the left. The white arrows indicate stops due to intramolecular cross-linking, and the black arrow indicates the stop due to an intermolecular cross-linked adduct. The identity of the U residue downstream from the cross-linked site is indicated. (**D**) RNaseH mapping of TB11Cs2C2 cross-linked species. (**a**) Cross-linking to srRNA-6. RNA from untreated cells (lane 1), after cross-linking (lane 2), after cross-linking but digested with RNaseH (lane 3). The RNA was digested with RNaseH in the presence of oligonucleotide prior to splint labeling. The RNA was subjected to splint labeling, and the products were separated on a 6% denaturing gel next to the pBR322 DNA-*Msp I* digest. The location of oligonucleotide binding and the distance between the cleavage site is given. (**b**) The same as in a but the analysis was performed using an oligonucleotide situated within srRNA-2.

adduct (U9) was revealed in the terminal stem. An adduct was also mapped at position U16, in a single stranded domain, suggesting a possible tertiary intramolecular interaction. Interestingly, a stop corresponding to position 53 (marked with a black arrowhead) was also observed (Figure 3C). This stop was not found in RNA extracted from the gel, but was only enriched in RNA purified by affinity-selection, suggesting that this stop represents an intermolecular cross-link and not an intramolecular one. This cross-linked position lies exactly in the

intermolecular duplex between TB11Cs2C2 and srRNA-6, depicted in Figure 3A. Note that an additional weak stop was observed one nt after the major stop, which results from reverse transcriptase stopping at the cross-linked site itself.

To gain further support for the proposed interaction between TB11Cs2C2 and its two targets, the cross-linked species between the snoRNA and rRNA were analyzed by RNaseH mapping. The snoRNA-associated rRNA species were tagged by the splint labeling technique. In this method, a primer complementary to TB11Cs2C2 carrying a run of 8 G nt at the 3′-end of the oligonucleotide was used as template to incorporate [α-^{32}P]-dCTP at the 3′-end of TB11Cs2C2 using the enzyme T7 DNA polymerase (Supplementary Figure S1). In such an experiment, we anticipate identifying cross-links between TB11Cs2C2 and the different rRNA species linked to it. Indeed, upon UV cross-linking and splint labeling, a major cross-linked species appeared at the top of the gel [Figure 3D (a and b), lanes 2]. To map the cross-linked adducts, the rRNA was first specifically digested by RNaseH and specific oligonucleotides to rRNA and pre-rRNA (depicted schematically in Figure 3D). After digestion, the digested fragments carrying TB11Cs2C2, were detected by splint-labeling using the snoRNA-specific oligonucleotide. The results in Figure 3D–a demonstrate that upon RNaseH cleavage, the level of cross-linked species migrating at the top of gel was reduced and two new species of sizes ~130 and 170 nt appeared. The ~130-nt fragment [marked as (1)] was most probably generated by cleavage of a species that was cross-linked to the srRNA-6 before processing, and was then processed by cleaving at the 3′-end of the srRNA-6. The ~170-nt fragment is most probably the result of cleavages at both the internal oligonucleotide as well as the oligonucleotide situated at ITS7 [marked as (2)]. The size on gel represents the size of the rRNA fragment and the size of cross-linked TB11Cs2C2. These data support the interaction of TB11Cs2C2 with srRNA-6. Validating the interaction of TB11Cs2C2 with srRNA-2 was even more important, since it is impossible to detect such interaction by primer extension because the interaction domain lies at the 3′-end of the snoRNA. The same methodology described in panel a, was used to demonstrate the association with srRNA-2. Upon cleavage, two species of 140 nt were detected by using an oligonucleotide situated within the srRNA-2 (Figure 3D-b). These species are most probably generated from cleavage of the mature srRNA-2 carrying the cross-linked molecules. The heterogeneity in size of the fragments may stem from heterogeneity at the 5′-end of srRNA-2.

The data presented in panel D support the interaction of TB11Cs2C2 with both rRNA targets. It is not known if these interactions take place simultaneously or sequentially.

snoRNAi suggests that TB11Cs2C2 snoRNA functions in processing of small rRNAs within the LSU rRNA coding region

Based on the putative interaction domain between TB11Cs2C2 and rRNA (Figure 3A and B), we examined if this RNA is involved in rRNA processing. To this end, the cell line carrying the silencing construct for TB11Cs2C2 was used. To identify rRNA processing defects that might exist in these cells, RT–PCR and RNase protection assays were performed. Cells silenced for NOP58 were used as a control to calibrate the defects in rRNA processing. NOP58 is a structural protein that binds to all C/D snoRNAs and is essential for the stability of the particles. We previously reported the silencing of this factor (22). Total RNA was prepared from uninduced cells and NOP58 silenced cells after 3 days of silencing. The levels of the precursors, internal transcribed spacer (ITS) or external transcribed spacer (ETS) of rRNA (schematically represented in Figure 4A), were measured by RT–PCR. The results (Figure 4B-a) demonstrate the accumulation of precursors for all the intergenic regions under conditions of NOP58 silencing, suggesting the C/D snoRNA family must participate in processing SSU, LSUα and LSUβ rRNA, but also in the cleavage of srRNAs. The same RT–PCR methodology was used to examine the defects in cells silenced for TB11Cs2C2. The results (Figure 4B-b) demonstrate increase in ITS5 and ITS7 levels in TB11Cs2C2-silenced cells. No other major changes were observed in the other ITS's, suggesting the TB11Cs2C2 functions in processing events required to release srRNA-2 and -6. Next, an RNase protection assay was used to examine the level of srRNAs and their precursors. Anti-sense RNA probes were synthesized to the different domains as depicted in Figure 4C, and the protected fragments of mature RNA and the precursor were examined in uninduced cells and after 3 days of silencing (Figure 4C). The results demonstrate major changes in the level of ITS5 and ITS7 precursors (boxed) accompanied by clear reduction in the level of LSUβ and srRNA-6 (boxed) rRNAs. No change in precursors was observed for ITS6, suggesting that TB11Cs2C2 most probably mediates the processing upstream of srRNA-2 and downstream of srRNA-6. These processing events therefore release srRNA-2 and -6 from the precursor. These results are in agreement with the bioinformatic predictions and AMT-UV cross-linking (Figure 3).

TB11Cs2C1 snoRNA may function in processing of SSU rRNA

TB11Cs2C1 is located between snR30 and TB11Cs2C2 in the same locus, as described above. This snoRNA is also very abundant (22). As stated above, this snoRNA is not involved in modification. To examine if TB11Cs2C1 may function in rRNA processing, a bioinformatic search described above was performed, to examine the potential interaction of this snoRNA with rRNA. The results, shown in Figure 5A and B, demonstrate two potential base-pair interactions; one within rRNA, as previously suggested (30), and one in the ETS close to the A0 cleavage site. To examine if these interactions take place *in vivo*, these potential associations were examined by AMT UV cross-linking, as described above. The RNA was subjected to affinity selection using an anti-sense biotinylated oligonucleotide complementary to

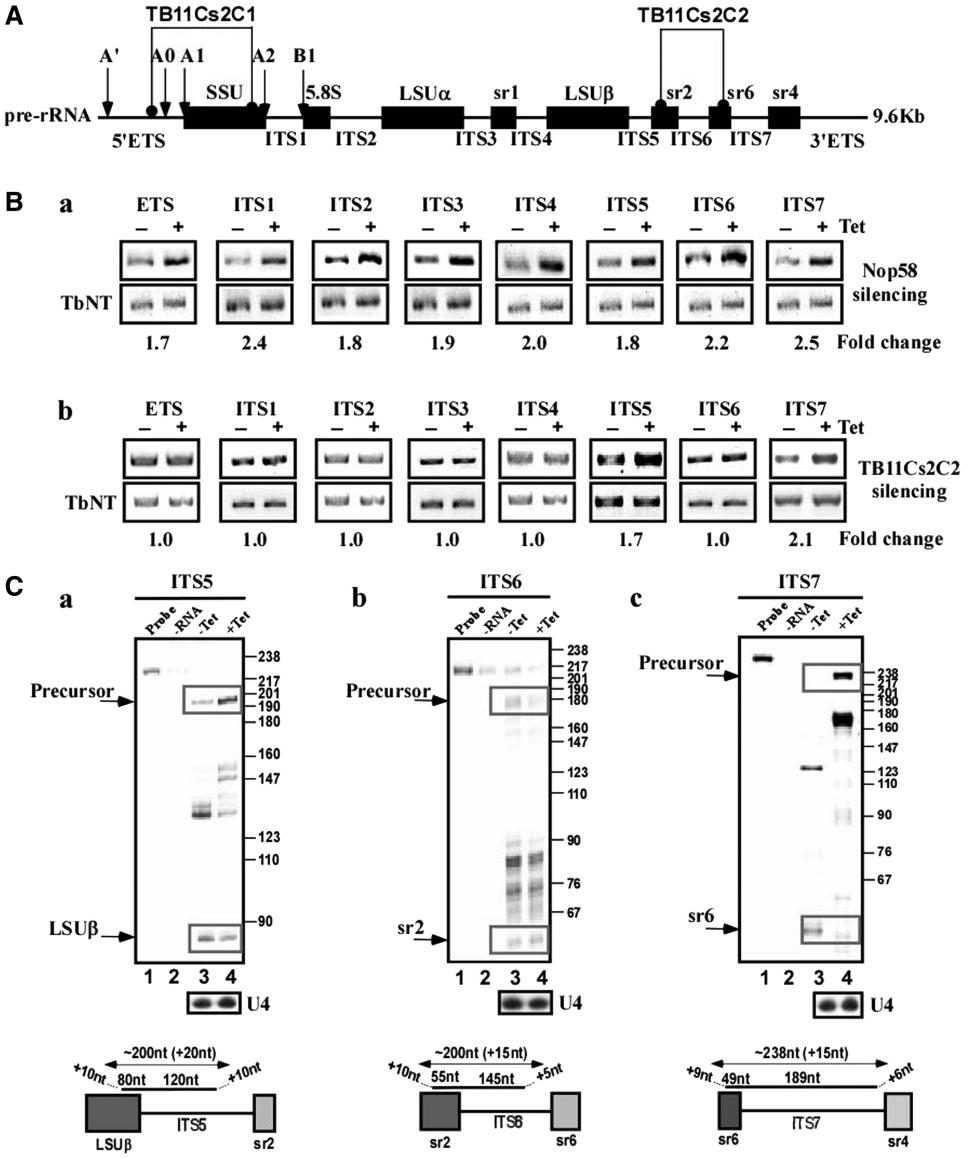

Figure 4. Functional analysis of TB11Cs2C2 snoRNA by RNAi. (**A**) Schematic representation of the pre-rRNA. The coding sequences are shown in black. The identity of the intergenic regions is given and the position of the cleavages is indicated. The proposed interaction domains of TB11Cs2C1 and C2 based on this study, are indicated. (**B**) RT–PCR comparing the rRNA processing defects under NOP58 silencing and TB11Cs2C2 silencing. RNA from uninduced cells or cells after 3 days of induction was used to prepare cDNA. cDNA was amplified with primers situated in the intergenic regions specified in Supplementary Data S1. The level of nucleoside transporter (TbNT) was used to normalize the level of RNA in each sample. The identity of the intergenic regions is indicated. (**a**) cDNA was taken from a cell line expressing the NOP58 silencing construct; (**b**) cDNA was prepared from cells expressing the TB11Cs2C2 silencing construct. The fold increase in the level of the intergenic region precursor is given below each panel. (**C**) RNase protection to detect accumulation of precursor, and reduction of mature rRNA. RNA from cells expressing the TB11Cs2C2 was used for RNase protection assay. The products were separated on a 6% denaturing gel. The structure of the anti-sense probe is schematically presented. The precursor and the mature snoRNAs are boxed. The sizes of the molecular weight marker (pBR322 DNA-*Msp*I digest) are indicated. In each panel: Lane 1, probe; lane 2, protection assay in the absence of RNA; lane 3, RNA from uninduced cells; lane 4, RNA from cells after 3 days of induction.

TB11Cs2C1. Primer extension performed on the SSU rRNA domain, using RNA extracted from UV irradiated cells and affinity selected with the snoRNA anti-sense oligonucleotide, indicated a cross-linked adduct on SSU rRNA at position U1900, further supporting the interaction between TB11Cs2C1 and SSU rRNA. The specificity of the cross-linking is evident, since the stop was eliminated following irradiation at 254 nm, which photoreversed the cross-linking (Figure 5C).

To evaluate the interaction with the ETS and TB11Cs2C1, we used the 'RNA walk' methodology that was recently developed in our group (41). The method is based on UV induced AMT cross-linking *in vivo* followed by affinity-selection of the hybrid molecules and mapping the intermolecular adducts by RT–PCR or real-time PCR. Domains carrying cross-linked adducts fail to efficiently amplify by PCR as compared with non-cross linked domains. To this end, RNA was prepared from the

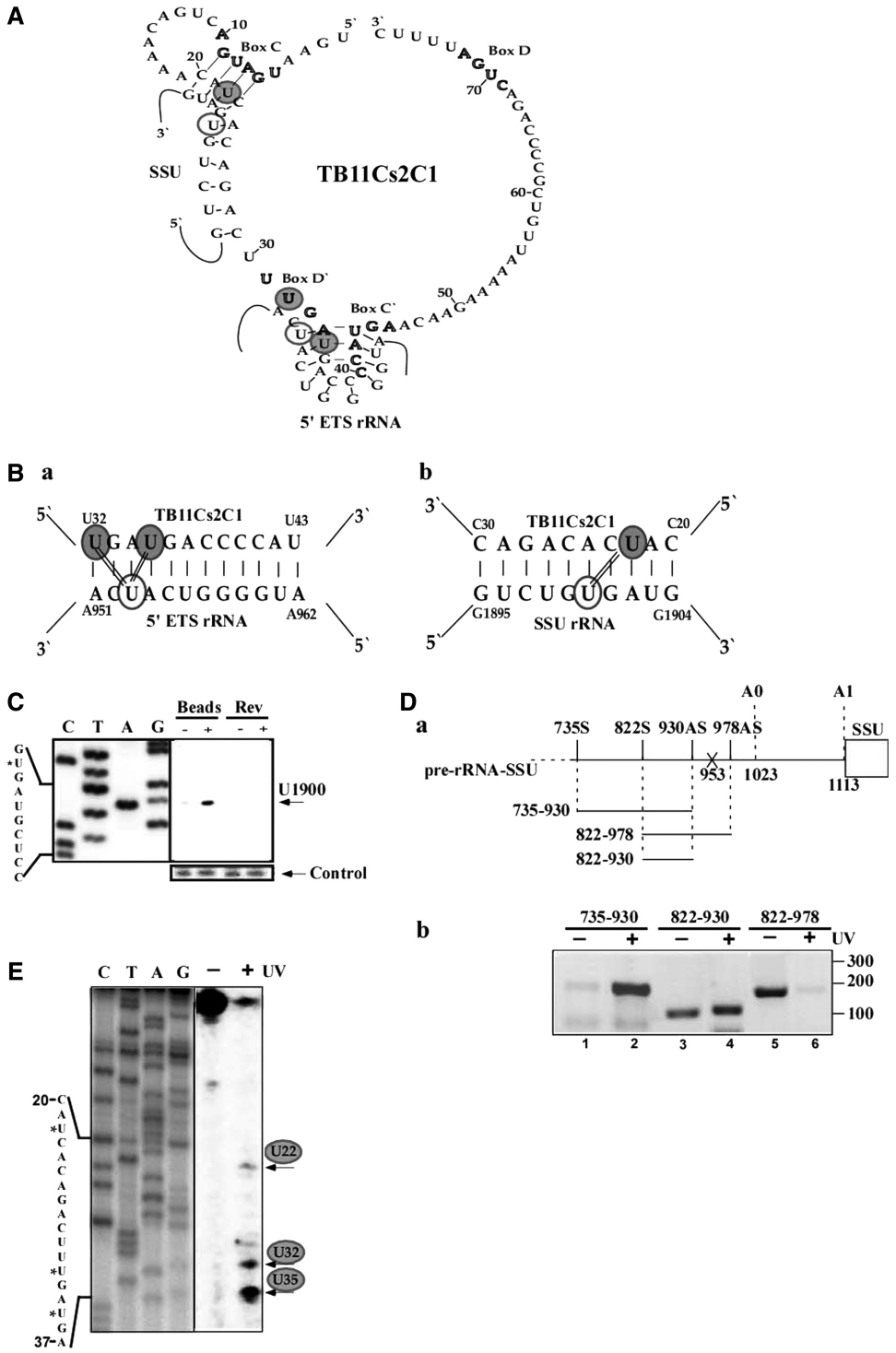

Figure 5. Potential interactions of TB11Cs2C2 snoRNA with rRNA. (**A**) The secondary structure of TB11Cs2C1. The base-pair interactions with the SSU rRNA and 5′-ETS sequences are presented. (**B**) Base-pair interaction between Tb11Cs2C1 and the target. The potential intermolecular cross-linked positions are circled. (**C**) Primer extension to map AMT adducts between TB11Cs2C1 and SSU rRNA. RNA from the affinity selected sample prepared from untreated cells or after AMT and UV cross-linking was taken for primer extension using a primer specified in Supplementary Figure S1. The extension was examined next to the DNA sequence of SSU rRNA in this domain. The sequence represents the RNA sequence (complementary to the cDNA synthesized). Cross linking was photoreversed by irradiation at 254 nm for 30 min, and the RNA was subjected to primer extension. To control for equal loading, a structural stop at a different position was compared. (**D**) Mapping the interaction domain of TB11Cs2C1 with 5′-ETS. (**a**) Schematic representation of the ETS domain. The positions of the primers used for amplification are indicated. X denotes the cross-linked position. (**b**) RT–PCR along the 5′-ETS. cDNA was prepared from the affinity selected RNA of untreated cells or after treatment with AMT and UV cross-linking. The cDNA was subjected to PCR using the set of primers indicated in panel a, and the PCR products were separated on a 1% agarose gel and stained with ethidium bromide. (**E**) Primer extension to map the AMT adducts on TB11Cs2C1. RNA derived from affinity selection of untreated cells (–UV) or after AMT and UV cross-linking, was extended with oligonucleotide complementary to the 3′-end of TB11Cs2C1. The products were separated on a 6% denaturing gel next to the DNA sequence of TB11Cs2C1 using the same primer. The sequence of this region is indicated.

cross-linked cells, and affinity purified with the anti-sense oligonucleotide to TB11Cs2C1. Following cDNA preparation using random primers, PCR was performed on the cDNA using three pairs of primers, as indicated in Figure 5D-a. The results in Figure 5D-b demonstrate that all domains were amplified from cDNA prepared from control cells. However, the fragment carrying the potential cross-linked domain could not be amplified when cDNA from the AMT UV cross-linking preparation was used, suggesting that this domain is cross-linked to rRNA. Interestingly, the other domains located on the pre-rRNA were more efficiently amplified after AMT-UV cross-linking and affinity selection (Figure 5D-b, compare lanes 2 and 4 with 1 and 3), since pre-rRNA is enriched by the affinity-selection procedure.

To verify that TB11Cs2C1 is indeed cross-linked at the relevant positions involved in interactions with the two targets, the affinity-selected RNA was used in primer extension with primer specific to TB11Cs2C1. The results suggest that primer extension stops were only observed in the affinity selected RNA at positions located within the TB11Cs2C1-rRNA interaction domains (Figure 5A and B). The adduct due to interaction with U22 results from cross-linking to SSU rRNA, whereas the adducts on U32 and U35 most probably result from interaction with the 5′-ETS. These data suggest that TB11Cs2C1 interacts with both SSU rRNA and pre-rRNA (5′-ETS), and therefore is most probably involved in SSU rRNA processing. The ultimate proof of the involvement of this snoRNA in rRNA processing could have been obtained by snoRNAi. However, we failed to obtain >45% reduction in the level of snoRNA in the silenced cells, and as a result of the inefficient knock-down, rRNA processing defects could not be detected. Only two kinds of snoRNAs exist, those that guide methylation and/or those that are involved in rRNA processing. The methylation that exists in the interaction domain of TB11Cs2C1 and SSU, is not guided by TB11Cs2C1 as previously shown (30), but is guided by TB9Cs2C4 (21) according to the +5 rule. This strongly suggests that TB11Cs2C1 is involved in rRNA processing of SSU.

DISCUSSION

In this study, the mechanism of snoRNAi was elucidated and was found to require both *Tb*AGO1 (Slicer) and *Tb*DCL2 (Dicer). The dependence on *Tb*DCL2 for snoRNAi stems from the localization of the target in the nucleolus.

The data obtained in this study are in agreement with a very recent study showing that the accumulation of transcripts from the CIR147 repeats in *T. brucei* is only slightly affected by *Tb*DCL1 knock-out, but requires *Tb*DCL2 activity (5). These repeats generate bona fide siRNAs harboring a 5′ monophosphate and a modified 3′-end (5). Like snoRNAs, CIR147 RNAs never leave the nucleus, and therefore their silencing depends on the nuclear Dicer isoform. It is possible that dsRNA produced by T7 RNA pol opposing constructs in the transgenic cells expressing the silencing construct for TB11Cs2C2 are transported to the cytoplasm and are digested to siRNAs by *Tb*DCL1. However, due to the absence of the target in the cytoplasm, these siRNAs would not be effective silencers. In order to mediate snoRNAi, siRNAs must be in the nucleus and interact with both AGO1 and the target snoRNA. Interestingly, in *ago1*$^{-/-}$ cells, CIR147 transcripts accumulate in the nucleolus, raising the intriguing possibility that silencing may take place in this compartment (8). The presence of the RNAi machinery in the nucleolus may explain why snoRNAi is so efficient.

It is currently unknown if snoRNAi has a physiological role, or if this mechanism simply takes advantage of the machinery that exists in the nucleus/nucleolus for silencing retroposons and the CIR147 transcripts (5). However, since we know so little about how snoRNAs are regulated and processed in the cells, it is still possible that snoRNAi has a physiological role in these processes. Interestingly, silencing of two small nuclear RNAs, namely telomerase RNA and 7SK RNA, was reported in mammalian cells using siRNAs. This suggests that DICER and AGO2 must also operate in the nucleus of mammalian cells to execute similar silencing (12).

This study also sheds light on the complex processing of rRNA in trypanosomes (Figure 4A). The cleavages that excise the SSU rRNA are different in trypanosomes as compared to other eukaryotes such as yeast and mammals (42). In trypanosomes, the first cleavage is between the SSU rRNA and 5.8S RNA at position B1, and only later do cleavages occur at positions A′, A0, A1 and A2 (43). In yeast and mammals, the cleavages to release the SSU rRNA first take place at A1 and A0, and only later do cleavages separate the SSU rRNA from 5.8S RNA (42). So far, only the U3 snoRNA was implicated in processing rRNA in the 5′-ETS domain of trypanosome rRNA (44,45). Another RNA that is implicated in processing of SSU rRNA is snR30, and this RNA was identified in the locus that also contains TB11Cs2C1 and TB11Cs2C2, described in this study (29). There are two additional snoRNAs that were shown to release the SSU rRNA in other eukaryotes, U14 (46) and U22 (47). Our bioinformatic searches failed to identify U14 and U22 homologs among the snoRNAs identified so far. TB11Cs2C1 has the potential to function in SSU rRNA processing, since it interacts with SSU rRNA at the 3′-end of the RNA as well as at a position upstream to A0. Although there is no structural resemblance between TB11Cs2C1 and U14, TB11Cs2C1 may nevertheless function as the functional trypanosome homolog of U14.

Interestingly, recent deep-sequencing analysis of small RNPs in *T. brucei* (Ullu and Michaeli unpublished results) identified highly abundant C/D molecules; these candidates most probably include previously unidentified snoRNA and/or snoRNA that carry out trypanosome-specific processing events. Work is in progress, using snoRNAi, to examine the distinct roles of these snoRNAs in rRNA processing.

The first snoRNA found to be involved in srRNA processing, TB11Cs2C2, was analyzed in this study. This

RNA has the potential to interact with both srRNA-2 and -6, and AMT-UV cross-linking performed in this study confirmed these interactions. The defects observed in rRNA processing suggest that this snoRNA may direct the cleavage upstream from srRNA-2 and downstream from srRNA-6. Interestingly, we did not observe accumulation of ITS6, located between srRNA-2 and srRNA-6, suggesting that there must be another snoRNA that mediates the cleavage of srRNA-2 from the precursor. Indeed, when the rRNA defects were examined in cells depleted for H/ACA RNAs via CBF5 silencing (29), a significant accumulation of ITS6 was observed, suggesting that there must exist an H/ACA RNA that is involved in trypanosome-specific rRNA processing at this site.

In summary, snoRNAi reflects the activity of the nuclear silencing machinery of trypanosomes, which most probably evolved to silence repeats and retroposons, but may have additional novel functions that have not been identified to date. However, snoRNAi can be utilized experimentally for functional analysis of nuclear/nucleolar ncRNAs. This study highlights the function of two abundant trypanosome snoRNPs, TB11Cs2C2, which functions in srRNA processing, and TB11Cs2C1, which is implicated in SSU rRNA processing, since it is no longer believed to function in rRNA methylation. TB11Cs2C1 may represent a functional homolog of snoRNA(s) found in other eukaryotes, which process rRNA at similar sites. The use of snoRNAi, together with deep-sequencing data, is expected to help identify additional trypanosome-specific snoRNAs in the near future.

SUPPLEMENTARY DATA

Supplementary Data are available at NAR Online.

FUNDING

Funding for open access charge: Israel-US Binational Science Foundation (BSF), by an International Research Scholar's Grant from the Howard Hughes Foundation to SM; Public Health Service Grant (grant number AI28798) to EU. S.M. holds the David and Inez Myers Chair in RNA silencing of diseases.

Conflict of interest statement. None declared.

REFERENCES

1. Ngo,H., Tschudi,C., Gull,K. and Ullu,E. (1998) Double-stranded RNA induces mRNA degradation in *Trypanosoma brucei*. *Proc. Natl Acad. Sci. USA*, **95**, 14687–14692.
2. Shi,H., Djikeng,A., Tschudi,C. and Ullu,E. (2004) Argonaute protein in the early divergent eukaryote *Trypanosoma brucei*: control of small interfering RNA accumulation and retroposon transcript abundance. *Mol. Cell. Biol.*, **24**, 420–427.
3. Shi,H., Tschudi,C. and Ullu,E. (2006) An unusual Dicer-like1 protein fuels the RNA interference pathway in *Trypanosoma brucei*. *RNA*, **12**, 2063–2072.
4. Shi,H., Tschudi,C. and Ullu,E. (2007) Depletion of newly synthesized Argonaute1 impairs the RNAi response in *Trypanosoma brucei*. *RNA*, **13**, 1132–1139.
5. Patrick,K.L., Shi,H., Kolev,N.G., Ersfeld,K., Tschudi,C. and Ullu,E. (2009) Distinct and overlapping roles for two Dicer-like proteins in the RNA interference pathways of the ancient eukaryote *Trypanosoma brucei*. *Proc. Natl Acad. Sci. USA*, **106**, 17933–17938.
6. Obado,S.O., Bot,C., Nilsson,D., Andersson,B. and Kelly,J.M. (2007) Repetitive DNA is associated with centromeric domains in *Trypanosoma brucei* but not *Trypanosoma cruzi*. *Genome Biol.*, **8**, R37.
7. Djikeng,A., Shi,H., Tschudi,C. and Ullu,E. (2001) RNA interference in *Trypanosoma brucei*: cloning of small interfering RNAs provides evidence for retroposon-derived 24-26-nucleotide RNAs. *RNA*, **7**, 1522–1530.
8. Patrick,K.L., Luz,P.M., Ruan,J.P., Shi,H., Ullu,E. and Tschudi,C. (2008) Genomic rearrangements and transcriptional analysis of the spliced leader-associated retrotransposon in RNA interference-deficient *Trypanosoma brucei*. *Mol. Microbiol.*, **67**, 435–447.
9. Kim,V.N., Han,J. and Siomi,M.C. (2009) Biogenesis of small RNAs in animals. *Nat. Rev. Mol. Cell. Biol.*, **10**, 126–139.
10. Durand-Dubief,M. and Bastin,P. (2003) TbAGO1, an argonaute protein required for RNA interference, is involved in mitosis and chromosome segregation in *Trypanosoma brucei*. *BMC. Biol.*, **1**, 2.
11. Liang,X.H., Liu,Q. and Michaeli,S. (2003) Small nucleolar RNA interference induced by antisense or double-stranded RNA in trypanosomatids. *Proc. Natl Acad. Sci. USA*, **100**, 7521–7526.
12. Robb,G.B., Brown,K.M., Khurana,J. and Rana,T.M. (2005) Specific and potent RNAi in the nucleus of human cells. *Nat. Struct. Mol. Biol.*, **12**, 133–137.
13. Kiss,T. (2002) Small nucleolar RNAs: an abundant group of noncoding RNAs with diverse cellular functions. *Cell*, **109**, 145–148.
14. Terns,M.P. and Terns,R.M. (2002) Small nucleolar RNAs: versatile *trans*-acting molecules of ancient evolutionary origin. *Gene Expr.*, **10**, 17–39.
15. Henras,A.K., Dez,C. and Henry,Y. (2004) RNA structure and function in C/D and H/ACA s(no)RNPs. *Curr. Opin. Struct. Biol.*, **14**, 335–343.
16. Meier,U.T. (2005) The many facets of H/ACA ribonucleoproteins. *Chromosoma*, **114**, 1–14.
17. Kiss-Laszlo,Z., Henry,Y., Bachellerie,J.P., Caizergues-Ferrer,M. and Kiss,T. (1996) Site-specific ribose methylation of preribosomal RNA: a novel function for small nucleolar RNAs. *Cell*, **85**, 1077–1088.
18. Ganot,P., Bortolin,M.L. and Kiss,T. (1997) Site-specific pseudouridine formation in preribosomal RNA is guided by small nucleolar RNAs. *Cell*, **89**, 799–809.
19. Tollervey,D. and Kiss,T. (1997) Function and synthesis of small nucleolar RNAs. *Curr. Opin. Cell Biol.*, **9**, 337–342.
20. Uliel,S., Liang,X.H., Unger,R. and Michaeli,S. (2004) Small nucleolar RNAs that guide modification in trypanosomatids: repertoire, targets, genome organisation, and unique functions. *Int. J. Parasitol.*, **34**, 445–454.
21. Liang,X.H., Uliel,S., Hury,A., Barth,S., Doniger,T., Unger,R. and Michaeli,S. (2005) A genome-wide analysis of C/D and H/ACA-like small nucleolar RNAs in *Trypanosoma brucei* reveals a trypanosome-specific pattern of rRNA modification. *RNA*, **11**, 619–645.
22. Barth,S., Shalem,B., Hury,A., Tkacz,I.D., Liang,X.H., Uliel,S., Myslyuk,I., Doniger,T., Salmon-Divon,M., Unger,R. *et al.* (2008) Elucidating the role of C/D snoRNA in rRNA processing and modification in *Trypanosoma brucei*. *Eukaryot. Cell*, **7**, 86–101.
23. Myslyuk,I., Doniger,T., Horesh,Y., Hury,A., Hoffer,R., Ziporen,Y., Michaeli,S. and Unger,R. (2008) Psiscan: a computational approach to identify H/ACA-like and AGA-like non-coding RNA in trypanosomatid genomes. *BMC Bioinformatics*, **9**, 471.
24. Doniger,T., Michaeli,S. and Unger,R. (2009) Families of H/ACA ncRNA molecules in trypanosomatids. *RNA Biol*, **6**, 370–4.
25. Cordingley,J.S. and Turner,M.J. (1980) 6.5 S RNA; preliminary characterisation of unusual small RNAs in *Trypanosoma brucei*. *Mol. Biochem. Parasitol.*, **1**, 91–96.
26. Schnare,M.N., Spencer,D.F. and Gray,M.W. (1983) Primary structures of four novel small ribosomal RNAs from *Crithidia fasciculata*. *Can. J. Biochem. Cell Biol.*, **61**, 38–45.

27. White,T.C., Rudenko,G. and Borst,P. (1986) Three small RNAs within the 10 kb trypanosome rRNA transcription unit are analogous to domain VII of other eukaryotic 28S rRNAs. *Nucleic Acids Res.*, **14**, 9471–9489.
28. Hartshorne,T. and Agabian,N. (1993) RNA B is the major nucleolar trimethylguanosine-capped small nuclear RNA associated with fibrillarin and pre-rRNAs in *Trypanosoma brucei*. *Mol. Cell. Biol.*, **13**, 144–154.
29. Barth,S., Hury,A., Liang,X.H. and Michaeli,S. (2005) Elucidating the role of H/ACA-like RNAs in trans-splicing and rRNA processing via RNA interference silencing of the *Trypanosoma brucei* CBF5 pseudouridine synthase. *J. Biol. Chem.*, **280**, 34558–34568.
30. Roberts,T.G., Sturm,N.R., Yee,B.K., Yu,M.C., Hartshorne,T., Agabian,N. and Campbell,D.A. (1998) Three small nucleolar RNAs identified from the spliced leader-associated RNA locus in kinetoplastid protozoans. *Mol. Cell. Biol.*, **18**, 4409–4417.
31. Wang,Z., Morris,J.C., Drew,M.E. and Englund,P.T. (2000) Inhibition of *Trypanosoma brucei* gene expression by RNA interference using an integratable vector with opposing T7 promoters. *J. Biol. Chem.*, **275**, 40174–40179.
32. Mandelboim,M., Barth,S., Biton,M., Liang,X.H. and Michaeli,S. (2003) Silencing of Sm proteins in *Trypanosoma brucei* by RNA interference captured a novel cytoplasmic intermediate in spliced leader RNA biogenesis. *J. Biol. Chem.*, **278**, 51469–51478.
33. Liang,X.H., Liu,L. and Michaeli,S. (2001) Identification of the first trypanosome H/ACA RNA that guides pseudouridine formation on rRNA. *J. Biol. Chem.*, **276**, 40313–40318.
34. Xu,Y., Liu,L., López-Estraño,C. and Michaeli,S. (2001) Expression studies on clustered trypanosomatid box C/D small nucleolar RNAs. *J. Biol. Chem.*, **276**, 14289–14298.
35. Liu,L., Ben-Shlomo,H., Xu,Y.X., Stern,M.Z., Goncharov,I., Zhang,Y. and Michaeli,S. (2003) The trypanosomatid signal recognition particle consists of two RNA molecules, a 7SL RNA homologue and a novel tRNA-like molecule. *J. Biol. Chem.*, **278**, 18271–18280.
36. Liang,X.H., Xu,Y.X. and Michaeli,S. (2002) The spliced leader-associated RNA is a trypanosome-specific sn(o) RNA that has the potential to guide pseudouridine formation on the SL RNA. *RNA*, **8**, 237–246.
37. Hury,A., Goldshmidt,H., Tkacz,I.D. and Michaeli,S. (2009) Trypanosome spliced-leader-associated RNA (SLA1) localization and implications for spliced-leader RNA biogenesis. *Eukaryot. Cell*, **8**, 56–68.
38. Dunbar,D.A., Wormsley,S., Lowe,T.M. and Baserga,S.J. (2000) Fibrillarin-associated box C/D small nucleolar RNAs in *Trypanosoma brucei*. Sequence conservation and implications for 2′-O-ribose methylation of rRNA. *J. Biol. Chem.*, **275**, 14767–14776.
39. Cimino,G.D., Gamper,H.B., Isaacs,S.T. and Hearst,J.E. (1985) Psoralens as photoactive probes of nucleic acid structure and function: organic chemistry, photochemistry, and biochemistry. *Annu. Rev. Biochem.*, **54**, 1151–1193.
40. Watkins,K.P., Dungan,J.M. and Agabian,N. (1994) Identification of a small RNA that interacts with the 5′ splice site of the *Trypanosoma brucei* spliced leader RNA in vivo. *Cell*, **T6**, 171–182.
41. Lustig,Y., Wachtel,C., Safro,M., Liu,L. and Michaeli,S. (2010) 'RNA walk' a novel approach to study RNA-RNA interactions between a small RNA and its target. *Nucleic Acids Res.*, **38**, e5.
42. Venema,J. and Tollervey,D. (1999) Ribosome synthesis in *Saccharomyces cerevisiae*. *Annu. Rev. Genet.*, **33**, 261–311.
43. Hartshorne,T. and Toyofuku,W. (1999) Two 5′-ETS regions implicated in interactions with U3 snoRNA are required for small subunit rRNA maturation in *Trypanosoma brucei*. *Nucleic Acids Res.*, **27**, 3300–3309.
44. Hartshorne,T. (1998) Distinct regions of U3 snoRNA interact at two sites within the 5′ external transcribed spacer of pre-rRNAs in *Trypanosoma brucei* cells. *Nucleic Acids Res.*, **26**, 2541–2553.
45. Hartshorne,T., Toyofuku,W. and Hollenbaugh,J. (2001) *Trypanosoma brucei* 5′ETS A'-cleavage is directed by 3′-adjacent sequences, but not two U3 snoRNA-binding elements, which are all required for subsequent pre-small subunit rRNA processing events. *J. Mol. Biol.*, **313**, 733–749.
46. Lange,T.S., Borovjagin,A., Maxwell,E.S. and Gerbi,S.A. (1998) Conserved boxes C and D are essential nucleolar localization elements of U14 and U8 snoRNAs. *EMBO J.*, **17**, 3176–3187.
47. Tycowski,K.T., Shu,M.D. and Steitz,J.A. (1994) Requirement for intron-encoded U22 small nucleolar RNA in 18S ribosomal RNA maturation. *Science*, **266**, 1558–1561.
48. Stern,M.Z., Gupta,S.K., Salmon-Divon,M., Haham,T., Barda,O., Levi,S., Wachtel,C., Nilsen,T.W. and Michaeli,S. (2009) Multiple roles for polypyrimidine tract binding (PTB) proteins in trypanosome RNA metabolism. *RNA*, **15**, 648–665.